

# A Simulated Assessment of Loading Effect on Buck-Boost Converters used in Maximum Power Point Tracking of Photovoltaic Systems

Barnam Jyoti Saharia<sup>1</sup>, Bani Kanta Talukdar<sup>2</sup>

Department of Electrical and Instrumentation Engineering, Assam Engineering College, Guwahati,  
Assam, India<sup>1,2</sup>

**Abstract:** This paper makes a comparative investigation resistive loading on buck-boost and its effect for use as interface for maximum power point tracking (MPPT) application in photovoltaic (PV) generators using the direct duty ratio control tracking algorithm. Analysis of the buck – boost converter has been undertaken to study the behaviour of the converter's performance with respect to the changing atmospheric conditions and in-turn duty ratio variation (as a result of MPPT) and the tracking efficiency of each converter. Effect of different resistive loads on the output of the converter side has also been considered for the same converter topology and it has been observed that the buck-boost converter is able to track the maximum power point (MPP) under variation of insolation, temperature and loading effect, with good tracking efficiency.

**Keywords:** PV, BUCK-BOOST converters, MPPT, Tracking efficiency, Hill climb algorithm

## I. INTRODUCTION

The photovoltaic (PV) generation system is one of the renewable energy sources that have attracted the attention of researchers in the recent decades due to its non-polluting, renewable and inexhaustible nature. There is an immense demand for finding feasible and environmental friendly renewable energy sources to meet the future energy requirements as fossil fuel reserves deplete. Solar energy is a viable substitute to fossil fuels among other available renewable energy sources such as wind, hydroelectric and geothermal power[1]. Solar PV generators have been used in small scale, stand-alone systems at low voltage levels as well as the high power installations, connected in grid mode and operating at medium or high voltage levels. The drawback of PV generators is its low conversion efficiency [2]. Efficiencies of typical crystalline PV cells are in the range of 12-18%, although experimental cells have been constructed that are capable of efficiency over 30%. The PV generators exhibit nonlinear current-voltage (I-V) and power-voltage (P-V) characteristics [3], a phenomenon that is more serious in partially shaded condition due to more than one maximum power point (MPP). For optimum use of PV generation, it is important to operate the system at the maximum available power production state for an available solar irradiation, temperature and load. Thus implementation of maximum power point tracking (MPPT) control techniques, in order to maximize the available output from a PV generator becomes an essential constituent of any PV system. The MPPT is the control algorithm to adjust the power interface (dc-dc converters) associated with the PV system such that greatest possible power yield is achieved, during moment to moment variations of insolation level, temperature and loads connected with the system.

A lot of researchers are associated with the development and design of a number of MPPT algorithms using

different techniques. Takashima *et al.* [4] uses curve fitting technique to calculate the operating point of the PV panel for a given value of insolation and temperature. Ibrahim *et al.*[5] discusses fuzzy logic and look-up table to identify the MPP locus of the PV panel. Masoum and Dehbonei [6] presents computational methods to model I-V characteristics of solar panels using mathematical equations or numerical approximations between solar cell open circuit voltage and cell short circuit current to calculate the MPP for different load conditions. Noguchi *et al.* [7] discusses short current pulse based adaptive MPPT for PV systems, such that proportional relationship between short current and optimum operating current of the PV panel finds use in order to determine the operating point for the maximum power output. Al. Atrash *et al.*[8] discusses statistical modelling of DSP based hill climbing (HC) MPPT algorithm with noisy environment. Liu and Lopes[9] present a new implementation of perturb and observe(P&O) MPPT algorithm which can mitigate the major drawbacks related to perturbation and observation model. Although very popular due to its simplicity and ease of implementation, P&O technique suffers from the drawbacks of having slow response speed, oscillations around the MPP in steady state and even at times tracking in wrong way under rapidly changing atmospheric conditions. Incremental conductance (IC) is able to overcome the problems associated with the P&O technique, provided the computations are carried out at fast rates. M.Miyatake *et al.*[10] uses search algorithm with Fibonacci sequence for MPPT control. The algorithm shows good performance of tracking even under partial shading effect. Artificial intelligence based algorithms using fuzzy logic controller, neural networks and adaptive neuro-fuzzy inference system (ANFIS) models is also put into practice for tracking the maximum operating power point of the PV panels [11-19]. Hohm and Ropp [20] make

a comparison of four low cost MPP tracking algorithms and reports that the P&O method if properly optimized can have efficiencies in excess of 97%. Esrarn and Chapman [21] compare various tracking algorithms and focuses in a comprehensive manner on the main differences between the different methods with respect to their PV array dependency, requirement of periodic tuning, their complexity of implementation, etc. A comparative study by Faranda and Leva[22] on ten widely used MPPT algorithms shows that the P&O method and IC method perform better than the rest of the algorithms. Eltawil and Zhao [23] present issues encountered in PV systems based on the grid side, demand side and PV side due to MPPT applications and includes possible countermeasures. Enrique *et al.*[24] presents the application of dc-dc converters as resistive emulators for tracking I-V and P-V characteristics.

The use of the converter as interface for MPPT for the majority of cases differs. In a good number of cases, a different converter topology in combination with a different tracking algorithm is used to track the MPP of a PV panel. Also the atmospheric condition subjected to the PV system to track the effectiveness of the MPPT algorithm is different in most studies. The PV panel used as well as the loads connected at the output side of the converter is also found to be diverse in many studies. In the absence of a uniform tracking algorithm, PV module and loads, it becomes difficult to predict with certainty the impact the converter interface has on the behaviour of the MPPT as well as the performance of the system as a whole. This paper takes into account the behaviour of the PV system deploying a MPPT algorithm subjected to a varying insolation and temperature profile using basic non-isolated dc-dc buck-boost converter. The tracking efficiency of the converter to meet a certain set of resistive loads is also studied and a comparative assessment of the performance of each of the converters is summarized. Liu *et al.*[25,26] and Sera *et al.* [27] note that HC and P&O technique is widely used with commercial systems due to its simple structure and few measured parameters involved in the tracking algorithm. For its simplicity and ease of implementation the HC technique of direct duty ratio control algorithm has been selected as the tracking algorithm in this paper.

Most investigations have been associated with the development, improvement and implementation of different tracking algorithms to achieve MPP operation. Under the changing condition of the irradiance and temperature, the operating power point of the PV panel changes leading the MPPT to change the duty ratio of the dc-dc converter interface such that it matches the operating point of the converter with the MPP of the PV panel.

However the study of the behaviour of the individual interfacing converters with respect to the variation of duty ratio in MPPT application is still an area that has not received the required focus of attention. It is important to note that the change in duty ratio has a corresponding

changing effect on the converter performance parameters, which may be in violation of the designed constraints of the converter topology such as ripple in inductor current and ripple in output voltage. In order to develop a PV power generation system with befitting converter topology that is able track the MPP operation, it is imperative that an analysis of the dc-dc converters used for this purpose and their performance with respect to tracking ability and behaviour with different loading demands is undertaken.

The paper is organised as follows. The introduction in section I is followed by the methodology implemented for the analysis in section II. This section comprises of the three subsections that discuss PV module modelling, the basic operation of dc-dc buck- boost converter and the MPPT algorithm implemented in this study. Section III summarises the results and discussion and section IV concludes with the findings of the study.

## II. METHODOLOGY IMPLEMENTED

### A. PV module modelling in software

A solar cell is basically a p-n junction fabricated in a thin wafer of semiconductor. The electromagnetic radiation of solar energy can be directly converted into electricity through the PV effect. When exposed to sunlight, photon with energy greater than the band-gap of the semiconductor creates the electron-hole pairs proportional to the incident radiation which is responsible for the generation of photocurrent.

Figure 1 shows the equivalent circuit of a PV cell. The current source  $I_{ph}$  represents the photocurrent.  $R_{sh}$  and  $R_s$  are the intrinsic shunt and series resistances of the cell respectively. Usually the value of  $R_{sh}$  is very large and hence they may be neglected to simplify the analysis.

Each PV cell, when grouped together in a combination of parallel and series cells constitute a PV module and PV arrays. Equations (1) – (4) are used for the modelling of the reference PV module KYOCERA KC120-1[7].

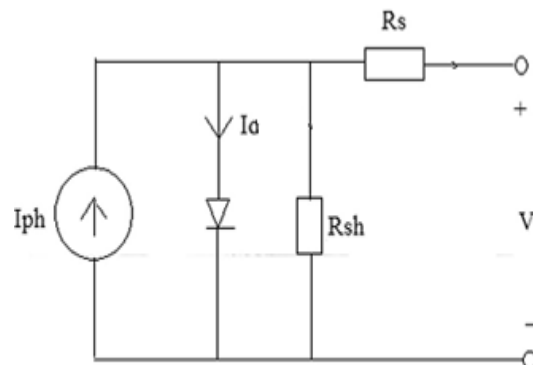


FIG.1. PV cell as a diode circuit

Module Photocurrent ( $I_{ph}$ ) is expressed by:

$$I_{ph} = [I_{scr} + K_i(T - 298)]\lambda / 1000 \quad (1)$$

Module reverse saturation current ( $I_{rs}$ ) is given by:

$$I_{rs} = I_{scr} / [\exp(qV_{oc} / N_s KAT) - 1] \quad (2)$$

The module saturation current ( $I_o$ ) varies with the cell temperature, which is expressed as:

$$I_o = I_{rs} [T / T_r]^3 \exp(qE_{go} / AK) \left[ \frac{1}{T_r} - \frac{1}{T} \right] \quad (3)$$

The current output of the PV module ( $I_{pv}$ ) is represented by:

$$I_{pv} = N_p I_{ph} - N_p I_o \left[ \exp\left\{ \frac{q(V_{pv} + I_{pv} R_s)}{N_s AKT} \right\} - 1 \right] \quad (4)$$

Where  $I_{scr}$  is the PV module short-circuit current(A) at  $1\text{kW/m}^2$  and  $25^\circ\text{C}$ ,  $K_i$  is the short-circuit current temperature co-efficient at  $I_{scr}$  ( $0.0017\text{A}/^\circ\text{C}$ ),  $T$  is the module operating temperature in Kelvin (K),  $\lambda$  is the PV module illumination ( $\text{kW/m}^2$ ),  $I_{rs}$  is the reverse saturation current of the module (A),  $q$  is Electron charge ( $1.6 \times 10^{-19}$  C),  $V_{oc}$  is the open circuit voltage of the PV panel (V),  $N_s$  is the number of cells connected in series in the PV module,  $k$  is Boltzmann's constant having the value of  $1.3805 \times 10^{-23}$  J/K,  $A$  is an ideality factor having value of 1.2,  $I_o$  is the PV module saturation current (A),  $T_r$  is the reference temperature in Kelvin ( $298$  K),  $E_{go}$  is the band gap for silicon having value of  $1.1$  eV,  $I_{pv}$  is output current of a PV module (A),  $V_{pv}$  is the output voltage of the PV module (V),  $N_p$  is the number of cells connected in parallel for the PV module. In the mathematical model the cells in series and the cells in parallel have values of  $N_s=36$  and  $N_p=1$ . Table II lists the electrical specifications of the Kyocera KC120-1 PV module [7] specified at standard testing conditions (i.e. at a irradiation of  $1000$   $\text{W/m}^2$ ,  $25^\circ$  C temperature and AM 1.5) which has been considered as the reference module in this paper for investigation. Figures 2 depicts the current voltage (I-V) and power voltage(P-V) characteristics of the simulated PV module at standard test conditions (STC) indicating that the model is able to predict accurately the PV module characteristics.

Table II. Electrical Characteristics of Kyocera KC120-1 PV model[7]

Parameter	Rating
Maximum Power	120 W
Voltage at maximum power	16.9 V
Current at maximum power	7.10 A
Short circuit current	7.45 A
Open circuit voltage	21.5 V
Total number of cells in series	36
Total no of cells in parallel	1
Band Energy	1.12 eV
Ideality factor	1.2

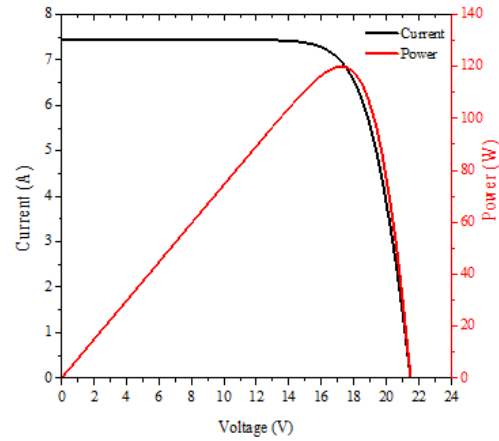


Fig 2: I-V and P-V curve of the PV module at  $1\text{kW/m}^2$  and  $25^\circ\text{C}$

### B. DC-DC Buck-Boost converter:

The voltage transformation in a dc-dc converter (switched mode) is done by controlling the operation of the switches. This is achieved by controlling the operation period, i.e. the on time ( $t_{on}$ ) and off time ( $t_{off}$ ) of the switches by PWM (pulse width modulation) technique.[30,31] The switching period  $T_s=t_{on}+t_{off}$  is held constant while the ratio of the on time to the switching time (i.e. duty ratio) is varied. In a PV system, the dc-dc converter is used to act as MPPT interface between the source and the load. The converter works to adjust its duty ratio (D) to match the requirements of the system. The duty ratio of a converter is defined as:

$$D = \frac{t_{on}}{T_s} \quad (5)$$

The steady state analyses of converters are governed by two fundamental laws, namely the volt-second balance and ampere-second balance, which decide the operation of dc-dc converters.[30,31]

Volt-second balance for inductor means that the product of the voltage and time in one period must be zero under equilibrium conditions which is expressed as:

$$\int_0^{T_s} V_L dt = 0 \quad (6)$$

Where  $V_L$  is the voltage across the inductor.

Ampere-second balance or charge balance for capacitor implies that the product of capacitor current and time should be zero under equilibrium condition which is described as:

$$\int_0^{T_s} i_c dt = 0 \quad (7)$$

Where  $i_c$  is the current through the capacitor.

Based on the above two laws, the input output relationship under steady state conditions can be obtained. However

some assumptions are made for the analysis namely, switches used in the converters are lossless, i.e. there is no on-state and off-state loss in the circuit, winding resistance in the inductor is zero, the equivalent series resistance of the capacitor is zero and the converters are 100% efficient. The governing equations of buck-boost converter is given in the Equations (8)

$$\frac{V_o}{V_{in}} = \frac{-D}{1-D} \quad (8)$$

Where  $V_{in}$  and  $V_o$  are input and output voltages of the converter respectively.

The main application of a step down/step up or buck-boost converter is in regulated dc supplies where a negative polarity output may be required with respect to the common terminal of the input voltage and the output may either be lower or higher than the input voltage as per requirement. The buck-boost converter can be obtained by the cascade connection of the two basic converters: the buck and the boost converter. The variation of the duty ratio determines if the converter operates as a buck or a boost converter.

### C. MPPT Algorithm Implemented

P&O technique is one of the most widely implemented tracking algorithms because of its simplicity, lower number of parameters involved and ease of implementation. HC method is quite similar to the P&O method. While the P&O method realizes the perturbation in voltage or current with the perturbation of power,[21] the HC method realizes the perturbation in the duty ratio with the change in power.

The direction of change in power correspondingly affects the next perturbation in the duty ratio. The flow chart of the HC algorithm used in the simulation study has been shown in Figure3. In this case, the perturbation in voltage along with power act as the input signals and the resultant output is the corresponding change in duty ratio by a fixed step  $\Delta D$  (designers choice of step) to match the maximum power point. As in this technique the perturbation leads to a direct change in the duty ratio, it is also sometimes called as the direct duty ratio technique of MPPT.

In order to track the MPP of the PV panel with solar radiation and temperature, the tracking effectiveness of the algorithm has been determined with the parameter tracking efficiency [20] ( $\eta$ ) for each of the converters which is defined as:

$$\eta = \frac{\int_0^t P_{inst}(t) dt}{\int_0^t P_{mpp}(t) dt} \quad (9)$$

Where  $P_{inst}$  is the instantaneous power at the operating point of the PV module and  $P_{mpp}$  is the instantaneous maximum power point of the PV module under given condition of insolation and temperature.

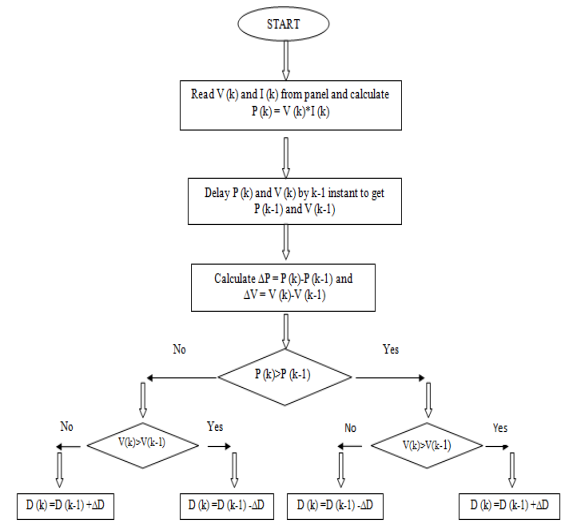


FIG.3. Flow chart of MPPT technique using HC method for direct duty ratio control

## III. RESULTS AND DISCUSSION

### A. MPP parameters performance

In order to study the effect of the variation of the change in external conditions of insolation and temperature on the PV module, a profile for solar insolation and temperature with operating range from 5 h to 18 h has been considered for investigation which is shown in Figure 4.

In preminent condition, the insolation reaches at level of  $1000 \text{ W/m}^2$  with temperature of  $31^\circ\text{C}$  at 13.36 h. The most pessimistic condition is observed at 17.36 h with an insolation level of  $100 \text{ W/m}^2$  with temperature of  $15^\circ\text{C}$ . I-V characteristics curve at both the conditions is shown in Figure 5.

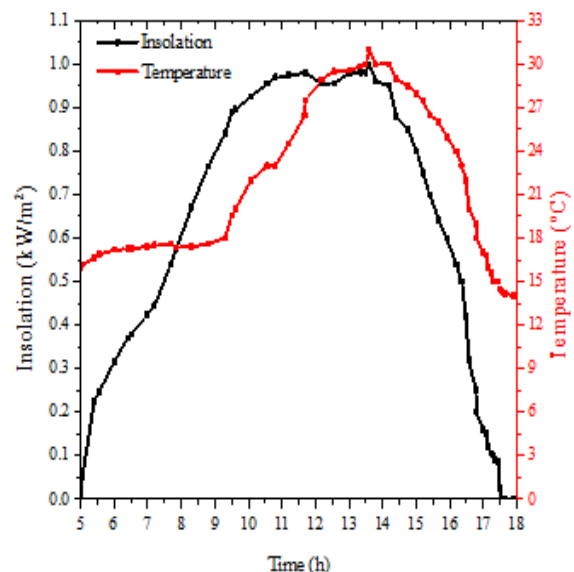


FIG.4. Insolation and temperature profile considered in the study

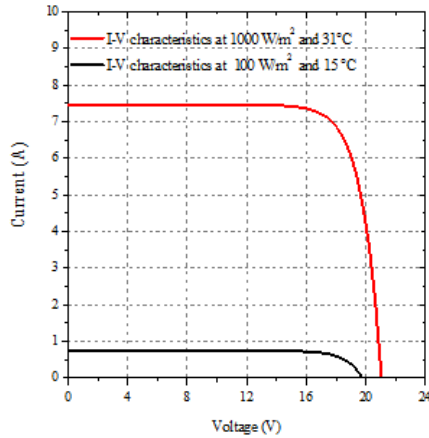


FIG.5. I-V characteristics of the PV module at two different conditions

The individual values obtained for maximum power point ( $P_{mpp}$ ), voltage at maximum power ( $V_{mpp}$ ), current at maximum power ( $I_{mpp}$ ) and the resistance at the maximum power point ( $R_{mpp}$ ) for the atmospheric conditions is shown in figures 6 and 7. The theoretical  $P_{mpp}$ ,  $V_{mpp}$ ,  $I_{mpp}$  and the corresponding  $R_{mpp}$  values are calculated for the analysis. The variation of  $V_{mpp}$  and  $I_{mpp}$  with the change in insolation and temperature has been shown in Figure 6.

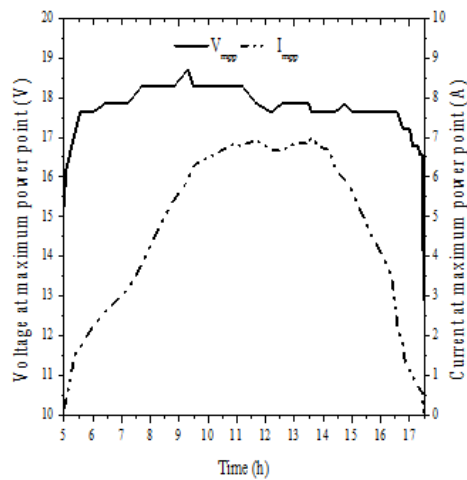


FIG.6. Variation of  $V_{mpp}$  and  $I_{mpp}$  for the changing insolation and temperature

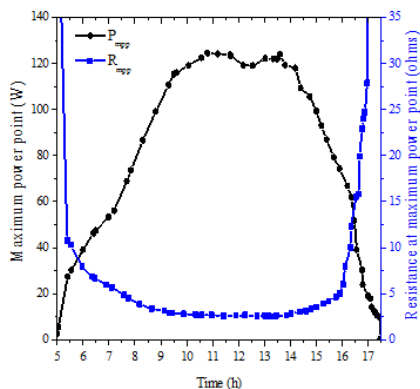


FIG.7. Variation of  $P_{mpp}$  and  $R_{mpp}$  for changing insolation and temperature

It is noticed that the variation in the current with insolation and temperature is almost linear, while there is very little change in the voltage with changing atmospheric conditions. The variation of  $P_{mpp}$  and corresponding change in  $R_{mpp}$  for the operating period is shown in Figure 7. This shows that with the decrease in panel resistance, power increases.

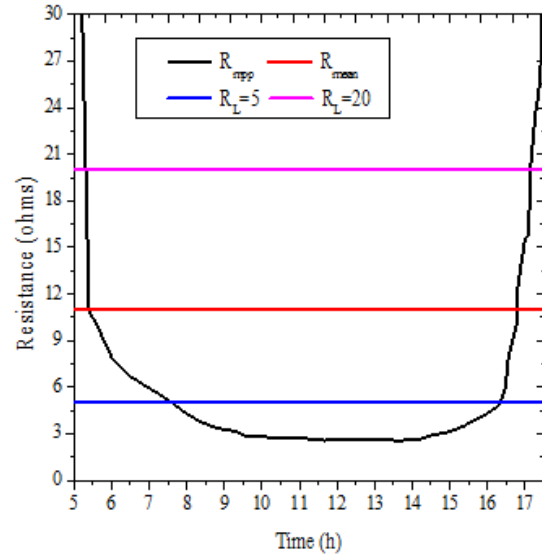


FIG.8. Resistance values considered for analysis of dc-dc converters

The mean value of  $R_{mpp}$  during the operating period is chronicled to be  $11.06\Omega$ . So for analysis of the different dc-dc converter topologies, two loads of  $20\Omega$  and  $5\Omega$  resistance, above and below the mean value are chosen as indicated in Figure 8.

### B. Optimal loading for DC-DC converters

This section involves testing the MPPT algorithm for varying loads for the same insolation and temperature profile that the converter is subjected to before. The investigation is undertaken to test under what values of resistive loading, buck-boost converter is seen to achieve maximum efficient tracking. The tracking algorithm employed for the analysis is the direct duty ratio tracking algorithm. The buck-boost converter is subjected to a set of resistive loads having values of  $5\Omega$ ,  $11\Omega$ ,  $20\Omega$  and  $25\Omega$ . Then the varying solar insolation and temperature profile is given as the input to the system, and the tracking efficiency is noted for each of the resistive sets of loadings. Figure 9 and figure 10 show the MPPT curve and the MPP tracking efficiency curve of buck-boost converter with different load resistance values.

From the simulation study it is seen that for a buck-boost converter the sets of resistive loads all shows the relatively higher tracking capability, following closely the MPP curve at almost all the conditions of insolation and temperature values. The tracking efficiency for buck-boost converter decreases for low insolation and temperature values, but it shows a better overall performance to tracking the load compared to the other two converters.

This ability of the converter to match with the  $R_i$  with the  $R_{mpp}$  makes this converter an ideal topology for MPPT applications.

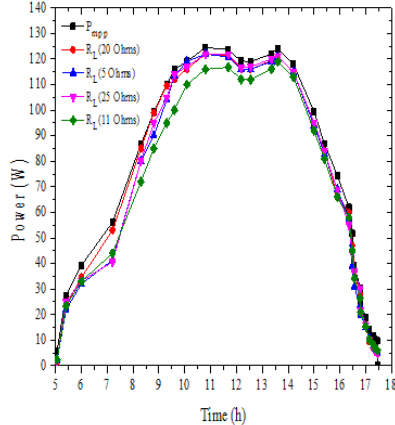


Fig 9. MPPT curve of buck-boost converter with different load resistance values

Thus we can safely say that to achieve most efficient tracking involving a buck-boost converter, the load connected at the output side of the converter can take any value within the range of resistances occurring at the preminent and pessimistic conditions. Moreover the overall tracking efficiency of this converter is also better when comparison is made for the buck and boost converter’s tracking effectiveness by the HC or direct duty ratio control MPPT algorithm.

Table III Average tracking efficiency of buck-boost converter for varying loads

Load	Tracking efficiency (%)
$R_L = 5 \Omega$	87.57
$R_L = 11 \Omega$	85.17
$R_L = 20 \Omega$	93.82
$R_L = 25 \Omega$	91.55

Table III list the average tracking efficiency of the buck-boost converter for different sets of resistive loads. Results for tracking efficiency of the algorithm reveals that the buck-boost converter gives adequate results. Thus signifying that with this converter topology, any load can be used to obtain better results for tracking efficiency.

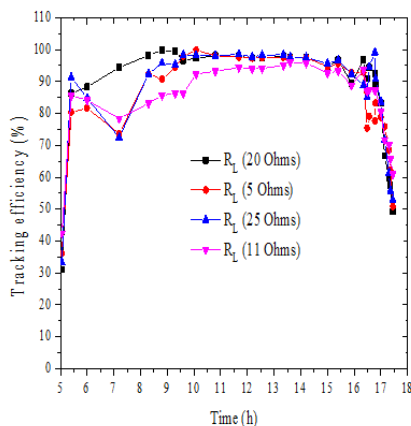


Fig 10. MPPT efficiency curve of buck-boost converter with different load resistance values

#### IV. CONCLUSIONS

From the tracking point of view, the converter is able to track the MPP with a relatively high efficiency for all the conditions that it is subjected to. This is because when PV panel impedance becomes high at pessimistic condition, the converter can act in buck mode and when the preminent conditions prevail, the converter switches to boost mode resulting in the reduction of the input impedance reflected by the converter and its ability to meet the converters’ MPP. Therefore, it can be inferred that the best converter topology that can be used as a power interface for MPPT application in PV generation is the buck-boost converter due to its improved tracking effectiveness and ability to track any load connected across it in PV power system applications.

#### REFERENCES

- [1] S.Sivasubramaniam, A. Faramus, R.D. Tilley and M.M. Alkaiji, “Performance enhancement in silicon solar cell by inverted nanopyrmaid texturing and silicon quantum dots coating,” Journal of Renewable and Sustainable Energy 6, 011204 (2014). doi 10.1063/1.4828364
- [2] L. Freris and D. Infield, Renewable Energy in Power Systems, (1st Edition, John Wiley & Sons, Ltd 2008). p.37
- [3] L.Liu, C. Liu and H. Gao, “A novel improved particle swarm optimization maximum power point tracking control method for photovoltaic array by using current calculated predicted arithmetic under partially shaded conditions,” Journal of Renewable and Sustainable Energy 5, 063139 (2013). doi 10.1063/1.4858615
- [4] T. Takashima, T. Tanaka, M. Amano and Y. Ando, “Maximum output control of photovoltaic (PV) array,” 35th Intersociety energy conversion engineering conference and exhibit (IECEC), Las Vegas, NV, 380-383 (2000).
- [5] H.E.S.A. Ibrahim, F.F. Houssiny, H.M.Z. El-Din and M.A. El-Shibini, “Microcomputer controlled buck regulator for maximum power point tracker for DC pumping system operates from photovoltaic system,” In 1999 IEEE International Fuzzy System Conference Proceedings; Seoul , South Korea. 406-11 (1999).
- [6] M. A. S. Masoum and H. Dehbonei, “Optimal power point tracking of photovoltaic system under all operating conditions,” In 17th Congress of world energy council, Houston TX (1998).
- [7] T. Noguchi, S. Togashi and R. Nakamoto, “Short-current pulse-based adaptive maximum power point tracking for a photovoltaic power generation system,” Elect. EngJpn. 139(1), 65 (2002).
- [8] H. Al-Atrash ,I. Batarseh and K. Rustom , “Statistical modeling of DSP-based hill- climbing MPPT algorithms in noisy environments,” In: Twentieth annual IEEE conference in Applied power electronics conference and exposition, APEC 2005,3, 1773-1777 (March 2005).
- [9] X. Liu, and L.A.C. Lopes, “An improved perturbation and observation maximum power point tracking algorithm for PV arrays,” In: Power electronics specialists conference, 2004, IEEE 35th annual Power electronics specialist conference 2004, PESC 04.3, 2005-2010 (2004).
- [10] M. Miyatake, T. Inada, I. Hiratsuka, H. Zhao, H. Otsuka and M. Nakano, “Control characteristics of a fibonacci-search-based maximum power point tracker when a photovoltaic array is partially shaded,” 4th International Conference on Power Electronics and Motion Control, IPEMC 2004, 816-821 (2004), ISBN 7-5605-1869-9.
- [11] A.AI-Amoudi and L. Zhang, “Application of radial basis function networks for solar-array modelling and maximum power-point prediction,” IEE Proceeding – Generation, Transmission and Distribution. 147(5),310–316 (2000). <http://dx.doi.org/10.1049/ip-gtd:20000605>
- [12] A.M.S. Aldobhani and R. John, “Maximum power point tracking of PV system using ANFIS prediction and fuzzy logic tracking,” Proceedings of the international multiconference of engineers and computer scientists IMECS, Hong Kong, vol. II., CD-ROM. Hong Kong: International Association of Engineers. (2008)
- [13] A. Iqbal, S.K.M. Ahmed, H. Abu-Rub, and S. Sinan, “Adaptive neuro-fuzzy inference system based maximum power point

- tracking of a solar PV module,” 2010 IEEE International Energy Conference & Exhibition, Energycon, Manama , 51-56 (2010).  
<http://dx.doi.org/10.1109/ENERGYCON.2010.5771737>
- [14] T. L. Kottas, Y.S. Boutalis, and A.D. Karlis, “New maximum power point tracker for PV arrays using fuzzy controller in close cooperation with fuzzy cognitive network,” *IEEE Transactions on Energy Conversion*, 21 (3), 793–803 (2006).  
<http://dx.doi.org/10.1109/TEC.2006.875430>
- [15] A. de Medeiros Torres, F.L.M. Antunes and F.S. dos Reis, “An artificial neural network-based real time maximum power tracking controller for connecting a PV system to the grid,” *Proceeding of IEEE the 24th annual conference on industrial electronics society*, 1, Aachen, 554–558 (1998).  
<http://dx.doi.org/10.1109/IECON.1998.724303>
- [16] A. Mellit, and S.A. Kalogirou, “Artificial intelligence techniques for photovoltaic applications: A review,” *Progress in Energy and Combustion Science*. 34(5), 574 (2008).  
doi:10.1016/j.peccs.2008.01.001
- [17] A. Mellit, et al., “Artificial intelligence techniques for sizing photovoltaic systems: A review,” *Renewable and Sustainable Energy Reviews*. 13, 406 (2008). doi:10.1016/j.rser.2008.01.006
- [18] S. Premrudeepreechacham and N. Patanapirom, “Solar-array modelling and maximum power point tracking using neural networks,” *IEEE Bologna power tech conference*, Bologna, Italy. (2003).  
<http://dx.doi.org/10.1109/PTC.2003.1304587>
- [19] H. Abu-Rub, A. Iqbal, et al., “Adaptive neuro fuzzy inference-based maximum power point tracking of solar PV modules for fast varying solar radiations,” *International Journal of Sustainable Energy*. 31(6),383 (2012). doi: 10.1080/1478646X.2011.587517
- [20] D.P. Hohm and M.E. Ropp, “Comparative study of maximum power point tracking algorithms,” *Progress in Photovoltaics: Research and Applications*.(11): 47-62 (2003).  
DOI:10.1002/pip.459
- [21] T. ESRAM and P.L. Chapman, “Comparison of photovoltaic array maximum power point tracking techniques,” *IEEE Trans. Energy Conver.* 22 (2), 439–449 (2007).  
<http://dx.doi.org/10.1109/TEC.2006.874230>
- [22] R. Faranda and S. Leva, “MPPT techniques for PV systems: Energetic and cost comparison,” *Power and Energy Society General Meeting - Conversion and Delivery of Electrical Energy in the 21st Century*, 2008 IEEE , Pittsburgh, PA , 1-6 (2008).  
<http://dx.doi.org/10.1109/PES.2008.4596156>
- [23] M. A. Eltawil and Z. Zhao, “MPPT techniques for photovoltaic applications.” *Renewable and Sustainable Energy Reviews*.25, 793 (2013).  
<http://dx.doi.org/10.1016/j.rser.2013.05.022>
- [24] J. M. Enrique, E. Durán, M. Sidrach-de-Cardona, J.M. Andújar, M.A. Bohórquez and J.E. Carretero, “A new approach to obtain I-V and P-V curves of PV panels by using DC-DC converters,” *Proceedings of the 31st IEEE Photovoltaic Specialist Conference, PVSC 2005, Orlando, EEUU*, 1769-1772 (2005).
- [25] F. Liu, S. Duan, F. Liu, B. Liu and Y. Kang , “A variable step size INC MPPT Method for PV systems,” *IEEE Trans. Indust. Electron.*55 (7), 2622–2628 (2008).
- [26] F. Liu, Y. Kang, Y. Zhang and S. Duan, “Comparison of P&O and hill climbing MPPT methods for grid-connected PV converter,” *In: IEEE Conference on Industrial Electronics and Applications*, Singapore, 804– 807 (2008).
- [27] D. Sera, T. Kerekes, R. Teodorescu and F. Blaabjerg, “Improved MPPT Algorithms for rapidly changing environmental conditions,” *In: IEEE Conference on Power Electronics and Motion Control*, Portoroz, 1614–1619 (2006).
- [28] N. Pandirajan and R. Muthu , “Mathematical Modeling of Photovoltaic Module with Simulink,” *In : Proceedings of the 1st International Conference on Electrical Energy Systems (ICEES’11)*, Newport Beach, CA , 3-5 January, 2011, 314-319 (2011).  
<http://dx.doi.org/10.1109/ICEES.2011.5725339>
- [29] Kyocera KC120-1 multi-crystalline photovoltaic module datasheet; 2001 ([www.kyocerasolar.com/assets/001/5180.pdf](http://www.kyocerasolar.com/assets/001/5180.pdf) ; last accessed on 12 February, 2014).
- [30] Umanand, *Power Electronics Essentials and Applications* (1st Edition, Wiley India, 2009)
- [31] M. Rashid, *Power Electronics – circuits, devices and applications* (3rd Edition, Pearson Education, 2004)